A tomographic infrared system for monitoring atmospheric pollution in urban areas

D. Giuli, F. Cuccoli, L. Facheris, S. Tanelli
Dipartimento di Ingegneria Elettronica - Università di Firenze
Via di S. Marta, 3 50139 Firenze - Italy

Abstract – This paper describes a feasibility study that has been carried out to define a measurement system able to estimate average concentration values of major species of pollutants over few km^2 areas. The system is based on laser diode semiconductor transmitters, and passive retroreflectors operating in the infrared region. Average concentrations are measured along rectilinear paths of 1 km maximum length, exploiting the infrared radiation absorption properties of pollutants. Measured data are then given as input to a tomographic reconstruction algorithm developed to retrieve space distribution of pollutants.

INTRODUCTION

In this paper we discuss the possibility to measure along rectilinear paths the average concentration of the fundamental molecular species of pollutants, with particular reference to CO, O_3 and nitrogen dioxides.This analysis was solicited by the fact that such measurement is the basis for the application of a tomographic reconstruction technique able to provide the distribution of concentration of pollutants. Such technique has been developed for rainfall field retrieval and tracking exploiting attenuation measurements along microwave links [1], nevertheless the data processing algorithm can be utilized unchanged for the problem discussed here. For a propagating electromagnetic wave with wavenumber ν (inverse of frequency) the Lambert-Beer law holds [2]:

$$dI(z,\nu)/dz = -\alpha(z,\nu)\cdot I(z,\nu) \qquad (1)$$

where $I(z,\nu)$ is the power spectral density (W/cm^2·Hz) at distance z along the wave propagation axis, and $\alpha(z,\nu)$ (cm^{-1}) is the attenuation coefficient, which is the sum of three terms:

$$\alpha = \alpha_R + \alpha_M + \alpha_G \qquad (2)$$

where α_R and α_M account for attenuation due to Rayleigh effect, and to Mie effect, respectively, while α_G accounts for attenuation due to molecular absorption:

$$\alpha_G(\nu,z) = \sum_{i=1}^{N} \sigma_i(\nu)\cdot N_i(z) \qquad (3)$$

where σ_i (in cm^2) and N_i (molecules per cm^3) are the absorption section and the concentration of the i-th molecular species, respectively. The molecular absorption is due to transitions between vibrorotational states that are peculiar of each molecular species. The characteristic frequency of each absorbing transition is the so-called absorption line. In standard pressure and temperature conditions (1 atm and 25°C, respectively) $\sigma_i(\nu)$ due to a single absorption line takes the typical Lorentzian form:

$$\sigma(\nu) = \frac{S}{\pi}\cdot\frac{\gamma_L}{(\nu-\nu_0)^2+\gamma_L^2} \qquad (4)$$

where ν_0 and γ_L are the center line wavenumber and width, respectively (cm^{-1}), and S the line amplitude (cm/molecule). The main molecular species of the atmosphere, be they pollutants or not, are characterized by a greater amplitude of the absorption lines in the wavelength interval 1-20 μm. The greater variability with wavelength of α_G, with respect to both α_R and α_M, is exploited for measuring the concentration of molecular species by means of the so called "derivative method" [2],[3].

2. The measurement method

If a transmitter emits a monocromatic radiation with power P_{r0}, the residual power P_r collected by a receiver at distance L is obtained by integrating Eq. (1) along a path of the same length. If $\overline{N}$ is the average concentration of the species of interest along the path of length L, and γ to account for all other attenuation effects, we have [2]:

$$P_r(\nu) = KP_{r0}(\nu)\cdot e^{-[\overline{N}L\sigma(\nu)+\gamma]} \qquad (5)$$

where K is the optical efficiency. Assuming that K and P_{r0} are independent of the wavenumber, the ratio between the derivative of Eq. (5) with respect to the wavenumber and Eq. (5) itself provides:

$$\frac{1}{p_r(\nu)}\frac{dP_r(\nu)}{d\nu} = -\left[\overline{N}L\frac{d\sigma(\nu)}{d\nu}+\frac{d\gamma}{d\nu}\right] \qquad (6)$$

If the wavenumbers are singled out for the species of interest, in correspondence of which the second term in the square parenthesis is negligible with respect to the first one, it is sufficient to perform power and power derivative measurements to obtain the average concentration along paths of known length.

3. The measurement apparatus

We describe here the measurement apparatus designed to directly provide an estimate of the left term of Eq.(6). The main devices that build up the proposed measurement apparatus are: infrared SDL (Semiconductor Diode Laser); passive retroreflector (corner cube reflector); infrared receiver; collimation and receiving electronics; electronic and control devices; pointing platform.

The average concentration measurement is performed by placing the devices according to the scheme of Fig. 2. The main reason for the adoption of semiconductor lasers as transmitters of infrared radiation are the following:

0-7803-3836-7/97/$10.00 © 1997 IEEE

- the emission line width (about 1MHz), is small enough to resolve the molecular absorption figures [3];
- the emission power under unimodal propagation (about 100μW), allows one to measure average concentrations for transmitter-receiver distances up to about 1 km;

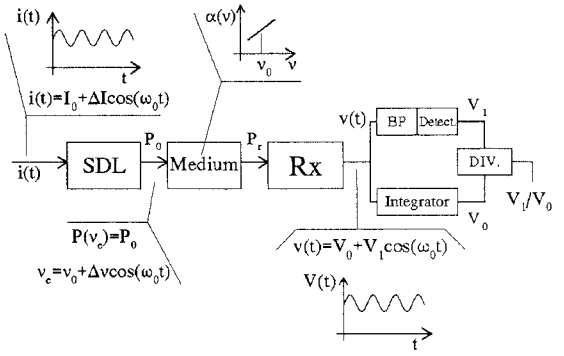

Fig. 1 - System configuration utilizable for measurements.

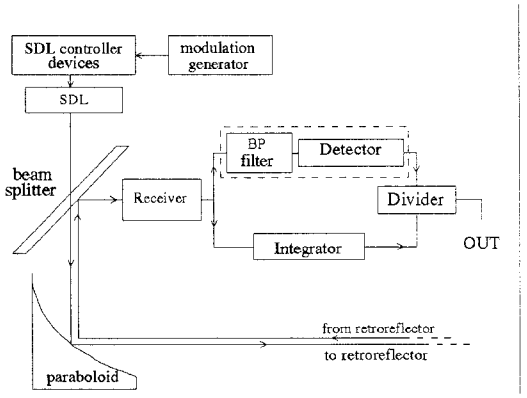

Fig. 2 - Arrangement of devices on the platform.

- the possibility to vary the emission frequency of the laser diode by means of the supply current allows one to measure the derivative of the received power [3]. The maximum value of the attenuation coefficient that still allows a significant power at the receiver's output was estimated based on SDL emission power, efficiency of the optical devices and effects of atmospheric turbolence [4] [5]. For 2 km two-way pathlength, a maximum attenuation coefficient has been estimated of about $2 \cdot 10^{-5}$ cm^{-1}. The left-hand quantity of Eq. (6) is measured (at the optimal wavelengths) by means of the scheme reported in Fig. 1. Therefore, the average concentration comes out to be:

$$\frac{1}{P_r}\frac{dP_r}{d\nu}\bigg|_{\nu_0} \propto \frac{V_1}{V_0} \quad \Rightarrow \quad \overline{N} \propto \frac{V_1}{V_0}$$

4. Optimal wavelengths

To exploit the apparatus described, it is necessary to single out as many wavelengths (meeting the requirements posed by the derivative method) as the number of species whose the average concentration measurement is desired. Based on the HITRAN database values [6] and on concentration values for the town of Florence provided by ARPAT-Italy, we searched for such optimal wavelengths by means of the characteristic parameters of the absorption lines (ν_0, γ_L and S), and of the minimum and maximum expected concentrations of the main molecules normally present in the atmosphere.

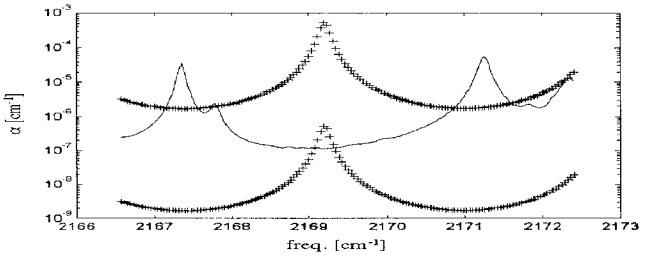

Fig. 3 Attenuation coefficient versus frequency (upper and lower + curves: due to 10 and 0.1 ppm CO concentration, respectively; continuous curve: due to all other molecules, at their maximum concentration)

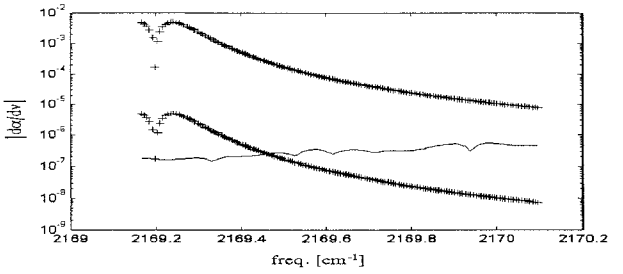

Fig. 4 Derivative of the absorption coefficient of Fig. 3, in the interval (2169.2,2170)cm^{-1}

Optimal wavelengths have been singled out for CO, O_3, N_2O, NO, NO_2. In particular, for CO we got the wavenumber interval (2169.2,2170)cm^{-1} (corresponding to the wavelength interval (4.608,4.609) μm). Concentrations ranging from 0.1 and 10 ppm can be measured in such interval. Fig. 3 shows that in such frequency interval the absolute value of the derivative of the attenuation coefficient due to CO is always prevailing with respect to the total contribution of the other species. When CO concentration is high, it is advisable to utilize wavenumbers greater than 2169.5cm^{-1}. Figs. 3 and 4 were obtained by accounting for the contribution of the lines of all molecules with their centre line frequency ν_0 included in the interval [2164,2174) cm^{-1}, that provide a significant level of absorption. As far as other molecules are concerned, we singled out an optimal frequency of 1057.77 cm^{-1} (9.454 μm) for ozone, 2240.41 cm^{-1} (4.45μm) for N_2O, 1900.04 cm^{-1} (5.26μm) for NO, 843.71 cm^{-1} (11.85μm) for NO_2.

5. Tomographic reconstruction of concentration fields

A network composed by an ensemble of transmitters, receivers and retroreflectors can provide a set of path-integrated attenuation measurements. These can be exploited as input to a

tomographic algorithm based on a stochastic approach, for which the reader is referred to [1]. Here we report synthetically some selected results.

For simulation purposes, we used the Gaussian Slender Plume model **[7]**. The model is valid under some quite restrictive conditions (see [7]); nevertheless, since the performance of the tomographic algorithm is practically independent of the field shape, the model served simply as reference to simulate plausible CO distributions due to point sources. The choice of CO is justified by the fact that its main sources (heating and internal combustion engines) can be modeled as point sources.

Two different network topologies were used. NET01, with 5 transmitter-receiver pairs and 5 retroreflectors, provides an excellent coverage of the surface to be monitored. NET02, instead, is designed to minimize the number of transmitter-receiver pairs, and consequently the cost of the entire network, (transmitters' costs are remarkably higher). Simulations refer to 40 point sources randomly located in a 200x200m square surface, 0.5m above ground. The amplitude of each source ranges between 0.1 and 0.5 g/s (e.g. 40 car engines running at minimum). We considered a horizontal 0.3m/s wind speed. The concentration field is developed over a 500x500 m square surface located 5m above the sources. The results are reported in Figs. 4 and 5. Errors have been computed referring to the the rectangular surface (strictly containing the measure network) plotted in the top-right frame of each figure. Notice that very low *me* values are observed in both cases; this is common to all simulations that have been performed. The spatial distribution is caught with appreciable fidelity; in particular, from the absolute error plots notice that zones with higher concentration are well individuated.

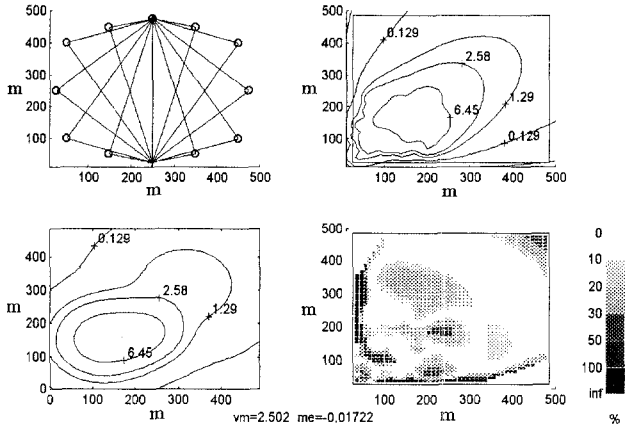

Fig. 4 - Reconstruction of a concentration of CO field (ppm) through NET01. Top left: measurement network; top right: simulated concentration field; bottom left: reconstructed concentration field; bottom right: error distribution; vm: mean value of reconstructed field; me: mean value relative error; +: transmitter-receiver pairs; o: retroreflectors

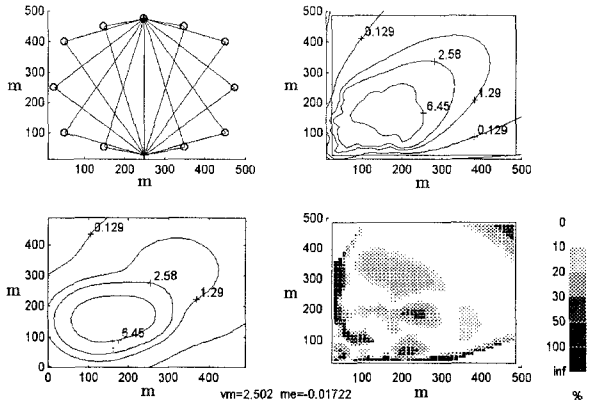

Fig. 5 - As Fig. 4, for NET02

6. Conclusions

The matter we have briefly synthesized in this paper is the result of a more general study that was carried out to assess the theoretical and technological feasibility of an air pollution monitoring system, which is particularly suitable for urban areas. Major difficulties were related to attenuation measurement principles and to their practical realizations, while the data processing algorithm for tomographic reconstruction was easily extended to the case under exam. The result is an affordable and flexible monitoring tool useful to provide, in particular if used jointly with a network of point sensors at ground, a complete and more reliable and detailed real-time information over the area.

References

[1] D. Giuli, L. Facheris, S. Tanelli: "Stochastic technique for 2D tomographic reconstruction of rainfall fields through microwave measurements" Proc. Mathematical Methods in Geophysical Imaging IV, Denver, Colorado, August 1996, pp. 129- 139.

[2] R.M. Measures "Laser remote sensing" Wiley Interscience, 1981

[3] R.T. Ku, E. D. Hinkley, J. O. Sample, 1975 : "Long-path monitoring of atmospheric carbon monoxide with a tunable diode laser system " Applied Optics, vol. 14, n. 4, pag. 854-861

[4] A. Ishimaru: "Wave propagation and scattering in random media" Academic Press, 1978

[5] H. Beaumont, 1996: "Caractérisation de la turbolence atmosphérique et procédure d'amélioration des images pour des observations horizontales au dessus de la mer" These de Doctorat présentèe au Département d'Astrophysique del'UniversitédeNice-Sophia Antipolis.

[6] L.S. Rothman: "AFGL trace gas compilation: 1982 version" Applied Optics, vol.22, n.11, pag. 1616-1625

[7] J.H. Seinfeld, 1986: "Atmospheric chemistry and physics of air pollution" Wiley Interscience